HHS Public Access

Author manuscript

Microcirculation. Author manuscript; available in PMC 2017 January 01.

Published in final edited form as:

Microcirculation. 2016 January ; 23(1): 75–87. doi:10.1111/micc.12261.

Macrophage recruitment and polarization during collateral vessel remodeling in murine adipose tissue

Scott A. Seaman[1], **Yiqi Cao**[1], **Chris A. Campbell**[2], and **Shayn M. Peirce**[1,2,*]

[1]Department of Biomedical Engineering, University of Virginia

[2]Department of Plastic Surgery, University of Virginia

Abstract

Objective—During autologous flap transplantation for reconstructive surgeries, plastic surgeons use a surgical pre-treatment strategy called “flap delay”, which entails ligating a feeding artery into an adipose tissue flap 10–14 days prior to transfer. It is believed that this blood flow alteration leads to vascular remodeling in the flap, resulting in better flap survival following transfer; however, the structural changes in the microvascular network are poorly understood. Here, we evaluate microvascular adaptations within adipose tissue in a murine model of flap delay.

Methods and Results—We used a murine flap delay model in which we ligated an artery supplying the inguinal fat pad. Although the extent of angiogenesis appeared minimal, significant diameter expansion of pre-existing collateral arterioles was observed. There was a 5-fold increase in recruitment of $CX3CR1^+$ monocytes to ligated tissue, a 3-fold increase in $CD68^+/CD206^+$ macrophages in ligated tissue, a 40% increase in collateral vessel diameters supplying ligated tissue, and a 6-fold increase in the number of proliferating cells in ligated tissue.

Conclusions—Our study describes microvascular adaptations in adipose in response to altered blood flow and underscores the importance of macrophages. Our data supports the development of therapies that target macrophages in order to enhance vascular remodeling in flaps.

Keywords

arteriogenesis; macrophage; adipose; collateral vessel

INTRODUCTION

The microvasculature is a dynamic system that changes its function and structure in response to biochemical and biomechanical stimuli. Prolonged ischemia, (e.g. the loss of blood flow to a region of tissue), is a particularly potent stimulus for angiogenesis, the formation of new blood vessels from pre-existing blood vessels[12,46,51] and arteriogenesis, the process by which pre-existing arteries/arterioles remodel to increase their diameter[17,20,40]. Angiogenesis and arteriogenesis are capable of restoring blood flow to ischemic tissue[40,41], providing injured tissue with the necessary nutrients to regenerate, and

*Corresponding author: Dr. Shayn M. Peirce, Ph.D., Professor, Department of Biomedical Engineering, University of Virginia, PO Box 800759, Health System, Charlottesville, Virginia 22908, Phone: 434-243-795, Fax: 434-982-3870, shayn@virginia.edu, Website: http://www.bme.virginia.edu/peirce/.

protecting against future ischemic damage[13]. While angiogenesis and arteriogenesis are physiological processes that occur in health (e.g. during exercise[6,37] and menstruation[11]) and during disease (e.g. in response to ischemic insult[17,20,40] and endometriosis[36]), the plastic surgery community has developed surgical strategies that presumably leverage these processes to aid in the repair of soft tissue defects through the use of autologous flaps.

Soft tissue defects commonly result from trauma, congenital disorders, or post-operative cancer resections[5]. Autologous flaps, which can be composed of fat, muscle, and/or skin, are surgically transferred from one region of the body to the site of the defect for reconstruction. Partial autologous flap loss due to inadequate blood flow can lead to multiple operations and a persisting defect. A pretreatment surgical technique termed “flap delay” involves the ligation of the main feeding vessel into the fat 10–14 days prior to tissue transfer to the recipient site. It is believed that this alteration in blood flow leads to growth and remodeling of the microcirculation, which allows for transfer of more tissue and improves autologous flap survival[22,30]. Although flap delay is performed routinely in the clinical setting and has been for many years, dating back to the first delayed flap for nasal reconstruction by Gaspare Tagliacozzi in the 16th century[38], the type of vascular remodeling that occurs within an autologous flap (angiogenesis, arteriogenesis, or both) and the types of vessels that undergo remodeling within the network (i.e. arterioles, capillaries, and/or venules) remain in question. Although the autologous flap is a composite tissue, the majority of the volume comes from the adipose tissue itself, and therefore a purely “adipose flap” will be the subject of our studies.

Prior studies have focused on the cellular composition and protein levels within an autologous flap, examining metabolic changes of the adipocytes, angiogenic protein secretion (VEGF, bFGF)[24], upregulation of hypoxia-inducible factor 1-α[9], and increased recruitment of endothelial progenitor cells[33]. Other studies have examined vessel dilation responses following vascular delay by using non-invasive laser Doppler flowmetry[3] and perfused tissue sections[8]; however, few studies to date have examined how the microvascular network dynamically and structurally adapts in concert with the immune cell compartment following ischemic ligation in a clinically relevant model of flap delay.

In this study, we investigated how the microvasculature in a purely adipose flap remodels – at the network level – in response to ischemic ligation of a feeding artery. By evaluating both angiogenesis and arteriogenesis, as well as immune cell recruitment in a published murine model of flap delay[46], our data show that arteriogenesis predominates over angiogenesis and that macrophages aid in the arteriogenic response following recruitment to the delayed adipose flap after 1–3 days. We examine the remodeling response at early time points to observe the interplay between immune cell recruitment and subsequent differentiation with the microvascular remodeling response. Understanding how the microvasculature of adipose tissue structurally adapts in response to ligation can suggest therapeutic mechanism(s) to further enhance autologous flap survival following flap delay, and improve long-term volume retention which will lead to better patient outcomes, fewer corrective procedures, and reduced cost burden on the healthcare system.

MATERIALS AND METHODS

Inguinal fat pad ligation surgery

All procedures were performed in accordance with the Institutional Animal Care and Use Committee of the University of Virginia. Eight to sixteen week old C57BL/6 mice were used for all studies, unless otherwise specified, with the number of mice denoted in figure legends. A modified, previously published inguinal fat pad ligation model[46] was used. Briefly, mice were anesthetized with ketamine/xylazine/atropine (60/4/0.2 mg/kg) and a 1.5 cm incision was made in the skin overlying the left inguinal fat pad using a scalpel blade (Figure 1). Skin and underlying connective tissue were carefully undermined using blunt dissection to expose the epigastric artery, which feeds the inguinal fat pad. The murine inguinal fat pad is a closed-network with one main feeding artery and typically three to four smaller collateral vessels that enter the lateral side of the fat pad from the skin (Figure 1A). A 10–0 nylon suture (Ethicon, Somerville, NJ) was used to ligate the epigastric artery after carefully separating the artery from its paired vein. The epigastric artery was severed following ligation, and loss of blood flow was confirmed visually using a surgical microscope under 3× magnification. The incision was closed with 8–0 nylon suture (Ethicon, Somerville, NJ). At subsequent time points (30 minutes, 12 hours, 24 hours, 72 hours), adipose tissue was harvested from euthanized mice, as described below. Sham surgery was performed on the contralateral side of each mouse. For the sham surgery, a 10–0 nylon suture was passed underneath the epigastric artery but was not tied, and the incision was closed with 8–0 nylon suture.

Intravascular perfusion of isolectin to visualize blood flow

The presence of flow in blood vessels was determined using intravascular perfusion of isolectin in Tie2-GFP reporter mice. Following ligation or sham surgery at specified time points (30 minutes, 12 hours, 24 hours, and 72 hours), the jugular vein was surgically exposed in anesthetized mice. 50 μg of Alexa Fluor 647 conjugated Isolectin GS-IB_4 from *Griffonia simplicifolia* (Life Technologies, Grand Island, NY) was suspended in 150 μL of sterile PBS (Life Technologies, Grand Island, NY) and drawn into a 28-gauge insulin syringe (Smiths Medical, Dublin, OH). The needle was carefully inserted into the jugular vein and the isolectin solution was slowly injected to prevent vessel rupture. Isolectin was allowed to circulate for 10 minutes, and then the mouse was humanely euthanized via CO_2 asphyxiation. Samples of the inguinal fat pad were harvested and whole-mounted for confocal microscopy, as described below.

Harvest of adipose tissue

Mice were euthanized via CO_2 asphyxiation. Mice were positioned supine, and all four paws were pinned to corkboard. A horizontal incision was made in the abdomen to expose the peritoneal membrane without puncturing. The skin was peeled back from the mouse to expose the subcutaneous inguinal fat pad. Areas of the inguinal fat pad or collateral vessels of interest were carefully excised. The “proximal” region was defined as the area of the inguinal fat pad immediately adjacent to where the epigastric artery enters the fat pad, the “distal” region was defined as the area adjacent to where the middle collateral vessel enters the inguinal fat pad, and the “distal” region was defined as the area of the adipose tissue

furthest from where the epigastric artery enters the fat pad (Figure 1). Adipose tissue and collateral vessels were immunostained for confocal microscopy or used in other assays, as described below.

Whole mounting and confocal imaging of excised adipose tissue

Harvested and immunostained samples of adipose tissue were allowed to adhere to gelatin coated microscope slides for 5 minutes. Slides were sealed with coverslips in 50:50 PBS/glycerol (Sigma-Aldrich, St. Louis, MO) solution. All fluorescently-labeled samples were imaged using a Nikon TE 2000-E2 microscope (Nikon instruments, Melville, NY) equipped with a Melles Griot Argon Laser System (Melles Griot Carlsbad, CA) and a Nikon D-Eclipse C1 confocal attachment. 40 μm Z-stacks with 2 μm step size were acquired of whole-mounted tissue to account for tissue depth. Magnification power varied from 10× magnification to 60× magnification and is indicated by scale bars on presented images. Multiple FOVs were acquired for each tissue, as listed for each study in the figure legend.

Quantification of isolectin perfusion in adipose microvessels

Separate images were taken for both the endogenous Tie2-GFP reporter (which labels blood vessels) and the intravascularly perfused isolectin (which labels blood vessels that have flow). 200× images (at least four unique FOVs per sample) were thresholded and converted to black and white to reduce background using ImageJ[35]. Images were then skeletonized so that each blood vessel was one pixel wide to account for differences in blood vessel caliber. The percent area of black pixels covering each image was calculated, and the ratio of the percent area of lectin perfused blood vessels to the percent area of the Tie2-GFP$^+$ blood vessels was calculated. A ratio of 1.0 is indicative of complete isolectin perfusion of the Tie2-GFP$^+$ blood vessels.

Microvessel network structural analysis

Samples of adipose from ligated and sham inguinal fat pads were harvested 3 days post surgery from the specified regions (proximal or distal) and fixed overnight in 4% PFA at 4°C. Samples were washed three times with PBS and submerged in 100 μL of 0.3% (v/v) Triton X-100/PBS for 3 hours at room temperature to permeabilize the tissue. Following permeabilization, the tissue was submerged in 100 μL of Alexa Fluor 568 conjugated isolectin diluted in 0.3% Triton X-100/PBS at 1:300. Samples were incubated in antibody solution on a rocker at 4°C overnight protected from light. Following staining, samples were washed five times for five minutes per wash with 0.3% Triton X-100/PBS. Samples were mounted on glass slides. Images (at least four unique FOVs per sample) were acquired using confocal microscopy. Images were acquired of regions that included only capillaries and excluded larger caliber vessels (e.g. arterioles and venules) to assess the extent of angiogenesis within the capillary bed specifically. A previously published MATLAB GUI, Rapid Analysis of Vessel Elements (RAVE)[42], was used to analyze blood vessel characteristics, specifically VLD and VVF.

In vitro angiogenesis sprouting assay

Tissue was harvested 3 days post surgery from ligated and sham inguinal fat pads at the specified regions (proximal and distal) in six mice. A previously published model for determining angiogenic capability[14] was used to assess the angiogenic capability of ligated and sham tissue. Briefly, six small ~1 mm^3 pieces of sample tissue were embedded into 40 μL Growth Factor Reduced BD Matrigel Matrix Phenol-Red Free (BD, Franklin Lakes, NJ). After Matrigel solidified, the plug was covered with 200 μL of Endothelial Cell Growth Medium (EGM-2, Lonza, Basel, Switzerland). Media was changed every other day. Four, 40× brightfield images of each adipose tissue explant were acquired using a Nikon TE 2000-E2 microscope, and the percent of explants exhibiting capillary sprouting were calculated. Explants were considered positive for sprouting when new capillary networks were observed on the periphery of the adipose tissue explant.

Quantification of collateral vessel diameter

Three days post surgery, five mice were euthanized via CO_2 asphyxiation and both left and right inguinal fat pads were surgically exposed, as described above. The collateral vessel entering the fat pad was located in the distal region of the fat pad. The fascia above the collateral vessel was removed to expose the vessel. The collateral vessel was carefully removed to retain structural integrity and was placed on a gelatin-coated slide. The collateral vessel was allowed to adhere for five minutes and the collateral vessel was encircled with a hydrophobic pen. 100 μL of 18.3 μM adenosine in Ringer's solution was superfused onto the vessel for five minutes to ensure vessels were maximally dilated, which allowed direct comparison between the collateral vessels of ligated and sham adipose tissues. Adenosine was aspirated, and 100 μL of 4% PFA was superfused onto the vessels. Vessels were stored in a hydrated petri dish overnight at 4°C.

Vessels were then immunostained to visualize the vascular smooth muscle cells, as follows. The PFA fixative solution was first aspirated and 100 μL of 5% (volume/volume) mouse serum in 0.3% Triton X-100/PBS was superfused for blocking and permeabilization of the vessel for 3 hours at room temperature. The blocking and permeabilization solution was removed, and 100 μL of monoclonal anti-actin, α-smooth muscle Cy3 (Sigma-Aldrich, St. Louis, MO, Clone 1A4) diluted in 5% mouse serum in 0.3% Triton X-100/PBS at 1:200 was added. Samples were incubated overnight at 4°C protected from light. Samples were washed five times with 0.3% Triton X-100/PBS for five minutes per wash. Slides were sealed with glass coverslips in 50:50 PBS/glycerol solution.

200× images of the collateral vessels were taken using confocal microscopy. Images included the feeding branch, the first branch in the adipose tissue, and the second branch in the adipose tissue. ImageJ was used to calculate the vessel diameters. Each individual sham diameter (e.g. 1st animal, 2nd branch, sham) was paired with the corresponding individual ligated diameter (e.g. 1st animal, 2nd branch, ligated) and a paired t-test was run.

CX3CR1-eGFP^{+} cell recruitment in inguinal fat

Three CX3CR1-eGFP mice crossed with NG2-DsRed mice were used for the monocyte and macrophage recruitment studies[7]. CX3CR1-eGFP cells consist mainly of monocyte-derived

macrophages, but dendritic cells and NK cells will also exhibit eGFP fluorescence[21]. Ligation or sham surgery was performed as described previously. 24 hours post-surgery, mice were anesthetized, and the jugular vein was surgically exposed. 50 μg of Alexa Fluor 647 conjugated Isolectin GS-IB_4 from *Griffonia simplicifoli* was injected into the jugular vein and was allowed to circulate for 10 minutes, as described above. Mice were euthanized via CO_2 asphyxiation. Samples of adipose were harvested at the distal location (described above) and whole-mounted for confocal imaging. 200× images (four FOVs per sample) were acquired with the collateral vessel centrally located in each image. CX3CR1-eGFP$^+$ cells located outside of the collateral vessels were quantified per field of view using ImageJ.

CD68$^+$ and CD206$^+$ macrophage quantification in inguinal fat

Ligation or sham surgery was performed as described above. Three days post-surgery, mice were humanely euthanized and samples of adipose tissue from the proximal and distal regions of each inguinal fat pad were harvested and fixed overnight in 4% PFA at 4°C. Samples were washed three times with PBS and submerged in 100 μL of 0.3% (v/v) Triton X-100/PBS for 3 hours at room temperature to permeabilize the tissue. Following permeabilization, the tissue was submerged in either (1) 100 μL of Alexa Fluor 488 conjugated isolectin (1:300) and Alexa Fluor 647 anti-mouse CD68 (AbD Serotec, Raleigh, NC, Clone FA-11) (1:200) diluted in 0.3% Triton X-100/PBS, or (2) 100 μL of Alexa Fluor 546 conjugated isolectin (1:300), Alexa Fluor 647 anti-mouse CD68 (AbD Serotec, Raleigh, NC, Clone FA-11) (1:200), and Alexa Fluor 488 anti-mouse CD206 (AbD Serotec, Raleigh, NC, Clone MR5D3) (1:200) diluted in 0.3% Triton X-100/PBS. Samples were incubated in antibody solution on a rocker at 4°C overnight protected from light. Following staining, samples were washed five times with 0.3% Triton X-100/PBS for five minutes per wash. Samples were mounted on glass slides. 200× images (at least four unique FOVs for each sample) were acquired using confocal microscopy, and CD68$^+$ and CD206$^+$ cells were quantified using ImageJ.

Quantification of proliferating cells

Samples of adipose tissue from the proximal and distal regions were acquired as described above under “Macrophage recruitment”. Tissue samples were submerged in 100 μL of Alexa Fluor 488 anti-mouse F4/80 (AbD Serotec, Raleigh, NC, Clone A3-1) (1:100), Alexa Fluor 546 conjugated isolectin (1:300), and Alexa Fluor 647 anti-mouse Ki-67 (Biolegend, San Diego, CA, Clone 16A8) (1:300) and diluted in 0.3% Triton X-100/PBS. Images were acquired using confocal microscopy as described above, and Ki-67$^+$ cells, as well as F4/80$^+$/Ki-67$^+$ cells, were quantified in ImageJ.

Statistical analysis

A two-way ANOVA or a Student’s t-test was performed, as indicated in each figure caption. Statistical significance was asserted at p-values < 0.05. All data are presented as average + standard deviation.

RESULTS

Surgical ligation eliminates blood flow through the epigastric artery but perfusion is recovered 72 hours after ligation

The reproducible vascular anatomy of the inguinal fat pad (Figure 1A) enabled us to study vascular remodeling in both the collateral vessels and in the vessels downstream of the ligation in the epigastric artery. To study vascular growth and remodeling in different regions of the inguinal fat pad, we divided it into two regions, relative to where the epigastic artery enters the fat pad: proximal and distal (Figure 1A). A macroscopic view of the inguinal fat pad (Figure 1B) shows the femoral artery, as well as the ligation site within the epigastric artery. Immunofluorescent staining for α-smooth muscle actin was performed to measure the diameter of the epigastric artery, which was roughly 150 μm (Figure 1C). Loss of blood flow downstream of the ligation site in the epigastric artery was visually confirmed following ligation, and in the contralateral fat pad undisturbed blood flow was visually confirmed following sham surgery.

Use of the Tie2-GFP reporter mouse allowed for visualization of arterioles, capillaries, and venules in the inguinal fat pad. Endothelial cells in these mice express GFP under the control of an endothelial-specific receptor tyrosine kinase (Tie2) promoter. Confocal micrographs of all samples revealed the expected lacy structure of the vascular network in the adipose tissue (Figures 2A, 2C, 2E, 2G). Intravascular perfusion of isolectin allowed for visualization of perfused vessels, and comparison with Tie2 expressing vessels in the same FOV (Figures 2B, 2D, 2F, 2H). We hypothesized that we would see a loss in perfusion surrounding the ligation site (proximal) immediately following ligation, but would observe a gradual increase in perfusion due to vessel remodeling in the distal region of the inguinal fat pad. We also hypothesized that there would be little to no alteration in the perfusion of the distal blood vessels where the collateral vessel enters. Representative confocal micrographs and quantification of images such as these revealed a near complete loss of perfusion in ligated tissue in the proximal region 30 minutes post-surgery (Figure 2B and 2I). Gradually and linearly over the next 72 hours, ligated fat pads experienced full recovery of perfusion (Figure 2H and 2I). In contrast, the ratio of perfused isolectin to Tie2-GFP expressing vessels in the sham fat pad maintained a relatively constant ratio close to 1.0, indicating no loss of perfusion following sham surgery (Figure 2I). Additionally, examination of confocal micrographs within the distal regions of the sham and ligated tissues (images not shown) and quantification of these images (Figure 2J), showed no alteration in perfusion in the distal regions of either sham or ligated tissues.

Vessel length density and volume vessel fraction are not affected by arterial ligation

An increased VLD and/or an increased VVF is indicative of angiogenesis. Therefore, to determine the extent of angiogenesis in the inguinal fat pad following surgical ligation of the epigastric artery, we used an automated image analysis program, RAVE to calculate VLD and VVF in samples obtained from different anatomical regions of the ligated and sham tissues. Images were acquired from isolectin stained, whole-mounted tissue. No significant difference in VLD or VVF was observed between ligated and sham tissue, irrespective of

the anatomical region (Figure 3A). We also compared the VVF between ligated and sham tissue based on anatomical region and saw no significant differences (Figure 3B).

Angiogenic sprouting capability is not affected by ligation

To test whether ligated tissue has a higher angiogenic capability than sham tissue, we used a previously published *in vitro* assay of functional angiogenic capability. Small pieces of adipose tissue (~1–2 mm^3) obtained from ligated and sham tissues were embedded into growth factor reduced Matrigel supplemented with endothelial growth media (Figure 3C). After 4–5 days endothelial sprouting and network formation were observed (Figure 3C). There was no significant difference in the percent of explants that exhibited endothelial sprouting between ligated and sham tissues (Figure 3D) regardless of the anatomical location from which the explants were harvested (Figure 3E). Consistent with the *en face* visualization of the capillary network, we did not observe an increase in vessel length density from the sprouts observed (Figure 3F,G) during the angiogenic capability assay from ligated tissue when compared to sham tissue.

Collateral vessel diameters enlarge following ligation

We were able to carefully excise the distal collateral vessel and keep it structurally intact for diameter measurement under maximal dilation (Figure 4A). We removed the collateral vessel from the animal so that we could measure diameter changes in the first and second branch within the inguinal fat pad, something that is not possible using intravital microscopy due to the opacity of the adipose tissue. The measurements were taken following adenosine dilation at the feeding vessel entering the inguinal fat pad, at the first branch, and at the second branch. Relative to the distal collateral vessel on the contralateral sham side, the ligated distal collateral vessel experienced a statistically significant increase in the vessel diameter (Figure 4B). The average percent increase from sham to ligated tissue was 56.9% for the feeding vessel, 38.7% for the first branch, and 41.3% for the second branch.

CX3CR1-eGFP monocyte recruitment is increased 24 hours post ligation

Monocyte recruitment to remodeling arterioles is a hallmark of arteriogenesis[18,39], and monocytes have been shown by our lab to extravasate from the venules as early as 6 hours post-ligation in skeletal muscle[7]. By using CX3CR1-eGFP mice crossed with NG2-DsRed mice and intravascularly perfusing isolectin, we were able to distinguish arterioles from venules[28] and examine the time course of recruitment of monocytes ($eGFP^+$ cells) to the remodeling tissue in the distal area of the inguinal fat pad. 24 hours after surgery, a statistically significant increase in CX3CR1-$eGFP^+$ cells was seen in the ligated tissue when compared to the sham tissue (Figures 5A, 5B). Quantification revealed an average of 68 $eGFP^+$ cells in the ligated tissue per FOV as compared to 10 $eGFP^+$ cells in the sham tissue per FOV after 24 hours (Figure 5C).

$CD68^+$ and $CD206^+$ cell recruitment is increased 72 hours post ligation

72 hours post-ligation, an increase in $CD68^+$ cells (i.e. macrophages[29]) was seen in the distal region of the ligated tissue (Figure 5D) when compared to the distal region of the sham tissue (Figure 5E). Quantification of the number of $CD68^+$ cells per FOV revealed that there

were roughly twice as many $CD68^+$ cells per FOV in the ligated distal tissue (113 $CD68^+$ cells/FOV) as compared to the sham distal tissue (66 $CD68^+$ cells/FOV) (Figure 5F). There was no significant difference in the number of $CD68^+$ cells in either the proximal region of the ligated tissue or the proximal region of the sham tissue (Figure 5F).

72 hours post-ligation, we observed an increase in the number of $CD68^+/CD206^+$ cells in the distal tissue when compared to the sham distal tissue (Figures 5G, 5H). We used CD206, the murine mannose receptor, coupled with the CD68 antibody to identify M2 polarized macrophages based on previous literature and studies[7,34,45,50]. Interestingly, the shape, size, and location of these CD68+/CD206+ cells were markedly different in ligated as compared to sham tissue. In ligated tissues, $CD68^+/CD206^+$ cells were much larger, as compared to the $CD68^+/CD206^+$ cells in sham tissue (Figure 5G, 5H). Moreover, $CD68^+/CD206^+$ cells in sham tissues were located on vessels, appearing to wrap around the capillaries, but in ligated tissues $CD68^+/CD206^+$ cells did not appear to be associated with or adjacent to blood vessels in this manner. Further, the $CD68^+/CD206^+$ cells in the ligated tissue were frequently present in pairs, which was an infrequent observation in sham tissue.

Ki-67^+ cells are increased in ligated tissue

To evaluate the number of proliferating cells, a cellular marker for entry into the active phases, Ki-67, was used. The Ki-67 protein is absent when cells are resting (G_0) and present when cells are in active phases (G_1, S, G_2, and mitosis). Seventy-two hours post-ligation, we observed an increase in Ki-67^+ cells in the distal region of the ligated tissue (Figure 5J) when compared to the distal region of the sham tissue (Figure 5K). Quantification revealed roughly six times more Ki-67^+ cells in the ligated distal tissue (average 39 Ki-67^+ cells) than in the sham ligated tissue (average 175 Ki-67^+ cells) (Figure 5L).

Co-labeling of excised ligated and sham fat pads with F4/80 and Ki-67 revealed enhanced co-localization of F4/80 and Ki-67 in ligated tissues compared to sham tissues, suggesting that macrophage proliferation is/was occurring. There were, on average, 63 $F4/80^+/Ki\text{-}67^+$ cells in ligated tissue per FOV with 45.4% of $F4/80^+$ cells also staining positively for Ki-67. In sham tissue, there were, on average, 8 $F4/80^+/Ki\text{-}67^+$ cells per FOV with 13.1% of $F4/80^+$ cells also staining positively for Ki-67. Co-localization of F4/80 and Ki-67, coupled with the timing of the $CD68^+/CD206^+$ recruitment to ligated tissue (72 hours), agrees with the notion that M2 macrophages are being recruited to ligated tissue where they are proliferating. Co-labeling with $CD68^+/CD206^+$ (Figure 5H) revealed enlarged, paired M2 macrophages, which may also be indicative of active cell proliferation.

DISCUSSION

Microvascular growth and remodeling in response to altered blood flow is an important adaptive response that has been widely studied in heart[39], skeletal muscle[7,13,15], and brain[16], among other organs. Far less is known about these processes in adipose tissue, despite the fact that the body's response to altered blood flow in skin, fat, and muscle is currently exploited in the clinical use of flap delay. The goal of our study was to examine structural adaptations of the microvasculature – at the network level – in response to altered blood flow in the murine inguinal fat pad. By using a combination of *in vitro* and *in vivo* assays,

we found that arteriogenesis, not angiogenesis, predominates in adipose three days after surgical ligation of the main feeding artery. Further, we found that CX3CR1$^+$ monocytes are actively recruited during collateral vessel diameter enlargement in fat. Localized proliferation of F4/80$^+$ cells around remodeling collateral arterioles in the inguinal fat pad 72 hours after ligation was synchronized with the observed increase in the number of CD68$^+$/CD206$^+$ cells, suggesting a potential role for macrophages in collateral vessel remodeling, as has been observed in other tissues[1,7,19,20].

Mechanisms of collateral vessel remodeling have been widely studied in skeletal muscle in the context of peripheral artery disease[48,52]. Briefly, it has been suggested that obstruction in blood flow causes a redistribution of blood flow through collateral vessels leading to alterations in the wall shear stress levels experienced by the vascular endothelium, which increases cytokine (e.g. monocyte chemotactic protein-1) production by endothelial cells[27,44]. Hypoxia and/or ischemia may also contribute to collateral vessel enlargement, as epicardial collateral vessel enlargement in the coronary circulation has been shown to occur in the absence of pressure gradients or wall shear stress changes following partial embolization in coronary arterioles[10]. Recruitment and activation of monocytes downstream of ischemia and/or hypoxia is an important process in collateral vessel enlargement. Our lab has recently shown that in murine skeletal muscle, monocytes extravasate from venules that are paired with collateral arterioles following ligation. Recruitment of monocytes, followed by elevated levels of CD68$^+$/CD206$^+$ macrophages, was associated with vascular smooth muscle cell proliferation in collateral arterioles and collateral vessel diameter expansion by 72 hours[7]. Our data collected in adipose tissue are consistent with these observations in skeletal muscle that implicate monocytes and monocyte-derived macrophages in collateral arteriole diameter expansion[7]. Here, we measured an increase in monocyte recruitment to the remodeling arteriole 24 hours post-ligation. We also observed a significant increase in CD68$^+$ macrophages and in CD68$^+$/CD206$^+$ macrophages in the ligated tissue when compared to the sham tissue three days post-surgery. This was accompanied by an increase in Ki-67$^+$ cells that were F4/80$^+$. Approximately 45% of F4/80$^+$ cells also stained for Ki-67 in ligated tissue as compared to 13% of F4/80$^+$ cells in sham tissue staining positive for Ki-67. Together, our findings suggest that monocyte-derived macrophages recruited from the circulation and proliferation of macrophages in the tissue play important roles in collateral vessel remodeling in adipose tissue. Whether or not F4/80$^+$ macrophages originated from recruited, monocyte-derived CX3CR1$^+$ cells and the extent to which these recruited cells overlap the CD68$^+$/CD206$^+$ macrophage population was not evaluated by our study. It is notable, however, that the observations we present here in murine adipose tissue mimic what has previously been observed in murine skeletal muscle[7]. We suggest that parallels in the time course of collateral vessel remodeling in muscle and fat may be related to the fact that the time course of the murine immune response and the diameters of the collateral vessels in both tissues are relatively equivalent, even though the metabolic demand between these tissue beds may differ substantially[49].

In our study, we observed diameter increase in the collateral arterioles that were consistent with previous studies involving the ligation of a feeder artery[4,13]. Moreover, we found that arteriogenesis – the diameter expansion of existing collateral arterioles due to structural remodeling of the vessel wall – predominated over angiogenesis in adipose tissue following

surgical ligation of the main feeding artery to the inguinal fat pad. The initiating stimulus in our model is still in question; we did not determine the extent to which hypoxia vs. wall shear stress changes contributed to the observed collateral enlargement in this model. In future work, it will be informative to measure wall shear stress in the collateral arterioles that experienced diameter enlargements, and to evaluate whether or not the adipose tissue becomes hypoxic after ligation.

While the role of angiogenesis in response to skeletal muscle ischemia appears to be essential, both in pre-clinical models and in clinical data studies[1,12,23,25], the role of angiogenesis in vessel adaptations to ischemia in adipose tissue remains unclear. Indeed, there is a dichotomy of findings from previous studies examining the role of angiogenesis and new blood vessel growth in adipose tissue – some studies cite an increase in angiogenesis, while others suggest no change or even a decrease[8,32]. Our studies in the murine inguinal fat pad agree with the latter – angiogenesis is not a major component of the adipose tissue's response to arterial ligation, at least within the first three days following ligation. We confirmed this finding with *in vitro* assays as well as *en face* visualization of the vascular network within the adipose tissue. It is possible that we did not observe an increase in angiogenesis because the collateral vessel's ability to rapidly remodel (three days) obviates the need for new capillary growth. Perhaps inducing a more severe degree of ischemia in the inguinal fat pad by ligating the femoral artery, similar to Suga et al.[46] (ligation of all collateral blood vessels), would provide a stimuli more inductive of angiogenesis. Adipose tissue has been shown to be tolerant of hypoxia (as evidenced by viable adipocytes in hypoxic, obese adipose tissue[47]) and has a lower resting metabolic demand when compared to skeletal muscle[49]. Both of these factors may mitigate the need for new capillary growth into adipose tissue, and may partially explain why we did not observe angiogenesis in our ligation model.

Our goal was to study the microvascular remodeling responses to vessel ligation in adipose tissue in order to better understand why there are improved clinical surgical outcomes associated with flap delay. However, our use of a murine model of flap delay makes several assumptions and oversimplifies the clinical flap delay procedure. For example, the composition and size of the flap that we examined was different than most surgical flaps used in clinical reconstructive surgery. While some surgical flaps consist solely of adipose tissue, most flaps are a composite tissue consisting of adipose tissue, muscle, and skin[26]. While our murine model is a simplification of the clinical scenario, we feel that our study can offer valuable insight because the adipose tissue component of flaps is the most voluminous part of the flap and is usually the main determinant of overall volume retention. Specifically, breast reconstructive flaps often consist entirely of adipose tissue and only a small amount of skin. We analyzed the remodeling response in the flap 1–3 days post-surgery rather than 10–14 days post-surgery as is practiced clinically and in previously published pre-clinical *in vivo* models[3,8] used to investigate flap delay. We chose earlier time points for our studies because we were interested in observing the transient recruitment of monocytes and macrophage differentiation (0–3 days) during the remodeling response that happen much sooner than the 10–14 days, which is the clinical time frame for flap delay. Notably, the size of the "flap" we used in our murine model was much smaller relative to the

flaps that are preconditioned with flap delay procedures in humans. The smaller size of our murine "flap" may protect it from oxygen diffusion limitations, and this may explain why we did not see a potent induction of angiogenesis in our studies. Moreover, it has been shown that the murine immune system differs quite substantially from the human immune system[43]; therefore, the analogous macrophage subpopulations in humans may be different from those studied here in mice. It may be possible to address some of the limitations of our study by performing future work in rat or rabbit models. We chose to use a published murine model because we made use of cell-type specific fluorescent reporters, which is difficult in rats or rabbits. However duplicating our study in a larger, more complex flap, such as the transverse rectus abdominis muscle flap[32,8], would allow for a better comparison to human flaps. Our study motivates future work that should examine how the enhancement and/or depletion of monocytes and macrophages affect collateral vessel remodeling in adipose tissue. Although our current studies focused on monocyte and macrophage recruitment to the remodeling adipose tissue, examining other cell types (T cells, B cells, dendritic cells and other monocyte subsets[31]) within the adipose tissue would be of value for future studies.

We feel that our studies add to the previous studies that examined flap delay in various pre-clinical models. While our animal model does not equate perfectly to the human anatomy that a plastic surgeon encounters when performing the flap delay procedure in the clinic, we believe that our findings highlight the importance of collateral vessel enlargement (arteriogenesis) over new vessel sprouting (angiogenesis). Our studies provide evidence that the remodeling response may initiate much sooner (within 1–3 days) than previously observed in other pre-clinical models[3,8] and clinically. This finding may be of potential interest to surgeons that are forced by clinical circumstance to perform the flap transfer procedure earlier than 14 days, as there may already be potential benefit from flap delay procedure at 1–3 days. We also provide a possible therapeutic mechanism (recruitment of anti-inflammatory macrophages) that may be targetable by pharmacological means[2].

A surgeon will evaluate several metrics of the flap prior to deciding which artery to ligate for the flap delay procedure. Based on the volume of the tissue that needs to be transferred, a surgeon will perform a more aggressive or less aggressive flap delay procedure. For very large volume flaps (~600–800 grams), a surgeon will try to ligate most of the feeding arterioles, but for small volume flaps (~200–300 grams) a surgeon will ligate only a few feeding arteries into the flap. The implicit rationale for this practice is that the extent of microvascular remodeling will be proportional to the extent of arterial ligation, and larger flaps will require more microvascular remodeling and hence more extensive ligations. However, the dose-response relationship between number of ligations and resulting arteriogenesis has not been explored. Although we do not directly address this in our study, our study shows that ligating even a single feeding artery can cause dramatic diameter expansion in smaller diameter collateral arterioles (e.g. 50 to 100 microns in diameter). Further, our data suggest that it is important to consider the remodeling responsiveness of smaller diameter arterioles that are capable of undergoing diameter enlargement. This is a particularly important finding, given the fact that in the clinical setting, these vessels are invisible to the surgeon and too small to be ligated but may be important contributors to the clinical benefit of flap delay.

In summary, our study closely examined the microvascular adaptations that occur in adipose tissue following ligation of a major feeding artery and provides potential cell targets (i.e. monocytes and macrophages) to enhance blood flow within delayed flaps. Understanding how the microvasculature of adipose tissue structurally adapts in response to surgically-induced ligation can suggest therapeutic mechanisms to further enhance flap survival following flap delay and may even eliminate the need for this pre-reconstructive surgical technique leading to fewer corrective procedures and reduced cost burden on the healthcare system.

ACKNOWLEDGEMENTS

The authors would like to thank Anthony Bruce for the management of the mouse colonies that were used. We also thank Dr. Song Hu, Dr. Patrick Cottler, and Dr. Norbert Leitinger for their insightful discussions and comments when planning and analyzing these studies.

SOURCES OF FUNDING

NIH T32GM008715 to S.A.S.; NIH EY022063, NIH HL082838, and The Hartwell Foundation to S.M.P.

LIST OF ABBREVIATIONS

VEGF	Vascular endothelial growth factor
bFGF	Basic fibroblast growth factor
GFP	Green fluorescent protein
PBS	Phosphate buffered saline
PFA	Paraformaldehyde
FOVs	Fields of view
VLD	Vessel length density
VVF	Volume vessel fraction
NG2	Neural/glial antigen 2

REFERENCES

1. Arras M, Ito WD, Scholz D, Winkler B, Schaper J, Schaper W. Monocyte activation in angiogenesis and collateral growth in the rabbit hindlimb. J. Clin. Invest. 1998; 101:40–50. [PubMed: 9421464]
2. Awojoodu AO, Ogle ME, Sefcik LS, Bowers DT, Martin K, Brayman KL, Lynch KR, Peirce-Cottler SM, Botchwey E. Sphingosine 1-phosphate receptor 3 regulates recruitment of anti-inflammatory monocytes to microvessels during implant arteriogenesis. Proc. Natl. Acad. Sci. U. S. A. 2013; 110:13785–13790. [PubMed: 23918395]
3. Aydin MA, Mavili ME. Examining microcirculation improves the angiosome theory in explaining the delay phenomenon in a rabbit model. J. Reconstr. Microsurg. 2003; 19:187–194. [PubMed: 12806581]
4. Bailey AM, O'Neill TJ, Morris CE, Peirce SM. Arteriolar remodeling following ischemic injury extends from capillary to large arteriole in the microcirculation. Microcirculation. 2008; 15:389–404. [PubMed: 18574742]
5. Bauer-Kreisel P, Goepferich A, Blunk T. Cell-delivery therapeutics for adipose tissue regeneration. Adv. Drug Deliv. Rev. 2010; 62:798–813. [PubMed: 20394786]

6. Bloor CM. Angiogenesis during exercise and training. Angiogenesis. 2005; 8:263–271. [PubMed: 16328159]
7. Bruce AC, Kelly-Goss MR, Heuslein JL, Meisner JK, Price RJ, Peirce SM. Monocytes are recruited from venules during arteriogenesis in the murine spinotrapezius ligation model. Arterioscler. Thromb. Vasc. Biol. 2014:1–11.
8. Cederna PS, Chang P, Pittet-Cuenod BM, Razaboni RM, Cram AE. The effect of the delay phenomenon on the vascularity of rabbit rectus abdominis muscles. Plast. Reconstr. Surg. 1997; 99:194–205. [PubMed: 8982203]
9. Ceradini DJ, Kulkarni AR, Callaghan MJ, Tepper OM, Bastidas N, Kleinman ME, Capla JM, Galiano RD, Levine JP, Gurtner GC. Progenitor cell trafficking is regulated by hypoxic gradients through HIF-1 induction of SDF-1. Nat. Med. 2004; 10:858–864. [PubMed: 15235597]
10. Chilian WM, Mass HJ, Williams SE, Layne SM, Smith EE, Scheel KW. Microvascular occlusions promote coronary collateral growth. Am. J. Physiol. 1990; 258:H1103–H1111. [PubMed: 2330998]
11. Demir R, Yaba A, Huppertz B. Vasculogenesis and angiogenesis in the endometrium during menstrual cycle and implantation. Acta Histochem. 2010; 112:203–214. [PubMed: 19481785]
12. Egami K. Ischemia-induced angiogenesis: role of inflammatory response mediated by P-selectin. J. Leukoc. Biol. 2006; 79:971–976. [PubMed: 16641139]
13. Mac Gabhann F, Peirce SM. Collateral Capillary Arterialization following arteriolar ligation in murine skeletal muscle. Microcirculation. 2010; 17:333–347. [PubMed: 20618691]
14. Gealekman O, Guseva N, Hartigan C, Apotheker S, Gorgoglione M, Gurav K, Tran K, Straubhaar J, Nicoloro S, Czech MP, Thompson M, Perugini RA, Corvera S. Depot-specific differences and insufficient subcutaneous adipose tissue angiogenesis in human obesity. Circulation. 2011; 123:186–194. [PubMed: 21200001]
15. Gruionu G, Hoying JB, Pries AR, Secomb TW. Structural Remodeling of the Mouse Gracilis Artery: Coordinated Changes in Diameter and Medial Area Maintain Circumferential Stress. Microcirculation. 2012; 19:610–618. [PubMed: 22587333]
16. Hecht N, He J, Kremenetskaia I, Nieminen M, Vajkoczy P, Woitzik J. Cerebral hemodynamic reserve and vascular remodeling in C57/BL6 mice are influenced by age. Stroke. 2012; 43:3052–3062. [PubMed: 22923448]
17. Heil M, Schaper W. Influence of Mechanical, Cellular, and Molecular Factors on Collateral Artery Growth (Arteriogenesis). Circ. Res. 2004; 95:449–458. [PubMed: 15345667]
18. Heil M, Ziegelhoeffer T, Pipp F, Kostin S, Martin S, Clauss M, Schaper W. Blood monocyte concentration is critical for enhancement of collateral artery growth. Am. J. Physiol. Heart Circ. Physiol. 2002; 283:H2411–H2419. [PubMed: 12388258]
19. Heil M, Ziegelhoeffer T, Wagner S, Fernández B, Helisch A, Martin S, Tribulova S, Kuziel Wa, Bachmann G, Schaper W. Collaretal Artery Growth (Arteriogenesis) after Experimental Arterial Occlusion Is Impaired in Mice Lacking CC-Chemokine Receptor-2. Circ. Res. 2004; 94:671–677. [PubMed: 14963007]
20. Helisch A, Schaper W. Arteriogenesis: the development and growth of collateral arteries. Microcirculation. 2003; 10:83–97. [PubMed: 12610665]
21. Jung S, Aliberti J, Graemmel P, Sunshine MJ, Kreutzberg GW, Sher A, Littman DR. Analysis of Fractalkine Receptor CX3CR1 Function by Targeted Deletion and Green Fluorescent Protein Reporter Gene Insertion. Mol. Cell. Biol. 2000; 20:4106–4114. [PubMed: 10805752]
22. Kerrigan C. Skin flap failure: pathophysiology. Plast. Reconstr. Surg. 1983; 72:766–774. [PubMed: 6647600]
23. Leblanc AJ, Krishnan L, Sullivan CJ, Williams SK, Hoying JB. Microvascular Repair: Post-Angiogenesis Vascular Dynamics. 2012; 19
24. Lineaweaver WC, Lei M-P, Mustain W, Oswald TM, Cui D, Zhang F. Vascular Endothelium Growth Factor, Surgical Delay, and Skin Flap Survival. Ann. Surg. 2004; 239:866–875. [PubMed: 15166966]
25. Marti, HH.; Risaut, W. Thrombosis and Haemostasis. Vol. 1999. Angiogenesis in ischemic disease; p. 44-52.

26. Mathes SJ, Nahai F. Classification of the Vascular Anatomy of Muscles: Experimental and Clinical Correlation. Plastic and reconstructive surgery. 1981; 67:177–187. [PubMed: 7465666]
27. Meisner JK, Price RJ. Spatial and Temporal Coordination of Bone Marrow-Derived Cell Activity during Arteriogenesis: Regulation of the Endogenous Response and Therapeutic Implications. Microcirculation. 2010; 17:583–599. [PubMed: 21044213]
28. Murfee WL, Skalak TC, Peirce SM. Differential arterial/venous expression of NG2 proteoglycan in perivascular cells along microvessels: identifying a venule-specific phenotype. Microcirculation. 2005; 12:151–160. [PubMed: 15824037]
29. Murray PJ, Wynn TA. Protective and pathogenic functions of macrophage subsets. Nat. Rev. Immunol. 2011; 11:723–737. [PubMed: 21997792]
30. Myers B, Cherry G. Causes of necrosis in pedicle flaps. Plast. Reconstr. Surg. 1968; 42:43–50. [PubMed: 4875691]
31. Ouchi N, Parker JL, Lugus JJ, Walsh K. Adipokines in inflammation and metabolic disease. Nat. Rev. Immunol. 2011; 11:85–97. [PubMed: 21252989]
32. Ozgentaş HE, Shenaq S, Spira M. Study of the delay phenomenon in the rat TRAM flap model. Plast. Reconstr. Surg. 1994; 94:1018–1024. discussion 1025–1026. [PubMed: 7972455]
33. Park S, Tepper OM, Galiano RD, Capla JM, Baharestani S, Kleinman ME, Pelo CR, Levine JP, Gurtner GC. Selective recruitment of endothelial progenitor cells to ischemic tissues with increased neovascularization. Plast. Reconstr. Surg. 2004; 113:284–293. [PubMed: 14707648]
34. Porcheray F, Viaud S, Rimaniol aC, Leone C, Samah B, Dereuddre-Bosquet N, Dormont D, Gras G. Macrophage activation switching: an asset for the resolution of inflammation. Clin. Exp. Immunol. 2005 0: 051006055454001.
35. Rasband WS. ImageJ.
36. Rogers PAW, Donoghue JF, Walter LM, Girling JE. Endometrial angiogenesis, vascular maturation, and lymphangiogenesis. Reprod. Sci. 2009; 16:147–151. [PubMed: 19001552]
37. Van Royen N, Piek JJ, Buschmann I, Hoefer I, Voskuil M, Schaper W. Stimulation of arteriogenesis; a new concept for the treatment of arterial occlusive disease. Cardiovasc. Res. 2001; 49:543–553. [PubMed: 11166267]
38. Santoni-Rugiu P, Sykes P. A History of Plastic Sugery. 2007
39. Schaper J, König R, Franz D, Schaper W. The endothelial surface of growing coronary collateral arteries. Intimal margination and diapedesis of monocytes - A combined SEM and TEM study. Virchows Arch. A Pathol. Anat. Histol. 1976; 370:193–205.
40. Schaper W, Scholz D. Factors regulating arteriogenesis. Arterioscler. Thromb. Vasc. Biol. 2003; 23:1143–1151. [PubMed: 12676799]
41. Schaper W. Collateral circulation: past and present. Basic Res. Cardiol. 2009; 104:5–21. [PubMed: 19101749]
42. Seaman ME, Peirce SM, Kelly K. Rapid analysis of vessel elements (RAVE): a tool for studying physiologic, pathologic and tumor angiogenesis. PLoS One. 2011; 6:e20807. [PubMed: 21694777]
43. Seok J, Warren HS, Cuenca AG, et al. Genomic responses in mouse models poorly mimic human inflammatory diseases. Proc. Natl. Acad. Sci. U. S. A. 2013; 110:3507–3512. [PubMed: 23401516]
44. Shireman PK. The chemokine system in arteriogenesis and hind limb ischemia. J. Vasc. Surg. 2007; 45:48–56.
45. Stein M, Keshav S, Harris N, Gordon S. Interleukin 4 potently enhances murine macrophage mannose receptor activity: a marker of alternative immunologic macrophage activation. J. Exp. Med. 1992; 176:287–292. [PubMed: 1613462]
46. Suga H, Eto H, Aoi N, Kato H, Araki J, Doi K, Higashino T, Yoshimura K. Adipose tissue remodeling under ischemia: death of adipocytes and activation of stem/progenitor cells. Plast. Reconstr. Surg. 2010; 126:1911–1923. [PubMed: 21124131]
47. Trayhurn P. Hypoxia and Adipose Tissue Function and Dysfunction in Obesity. Physiol. Rev. 2013; 93:1–21. [PubMed: 23303904]
48. Troidl K, Schaper W. Arteriogenesis versus angiogenesis in peripheral artery disease. Diabetes. Metab. Res. Rev. 2012; 28:27–29. [PubMed: 22271719]

49. Wang Z, Ying Z, Bosy-Westphal A, Zhang J, Schautz B, Later W, Heymsfield SB, Müller MJ. Specific metabolic rates of major organs and tissues across adulthood: Evaluation by mechanistic model of resting energy expenditure. Am. J. Clin. Nutr. 2010; 92:1369–1377. [PubMed: 20962155]

50. Willenborg S, Lucas T, van Loo G, Knipper Ja, Krieg T, Haase I, Brachvogel B, Hammerschmidt M, Nagy A, Ferrara N, Pasparakis M, Eming Sa. CCR2 recruits an inflammatory macrophage subpopulation critical for angiogenesis in tissue repair. Blood. 2012; 120:613–625. [PubMed: 22577176]

51. Xiong Y, Mahmood A, Chopp M. Angiogenesis, neurogenesis and brain recovery of function following injury. Curr. Opin. Investig. Drugs. 2010; 11:298–308.

52. Ziegler M, Distasi M, Bills R, Miller S, Alloosh M, Murphy M, George Akingba A, Sturek M, Dalsing M, Unthank J. Marvels, Mysteries, and Misconceptions of Vascular Compensation to Peripheral Artery Occlusion. Microcirculation. 2010; 17:3–20. [PubMed: 20141596]

PERSPECTIVES

Autologous adipose tissue grafting is being increasingly used to correct soft tissue trauma defects, congenital disorders, and disease resections, but resorption of grafted adipose tissue is high and unpredictable due to supposed improper vascularization. This study examines microvascular remodeling and macrophage recruitment in adipose tissue following ligation of the epigastric artery feeding the inguinal fat pad. We show that macrophage recruitment and synchronized arteriogenesis are responsible for microvascular changes within the adipose tissue. While macrophage polarization and collateral diameter expansion/arteriogenesis following induced ischemia have been studied extensively in skeletal muscle, we are the first to study these processes in adipose. We hope that this paper will serve as a platform for new studies examining microvascular remodeling within adipose tissue and ultimately improve grafted adipose tissue retention rates.

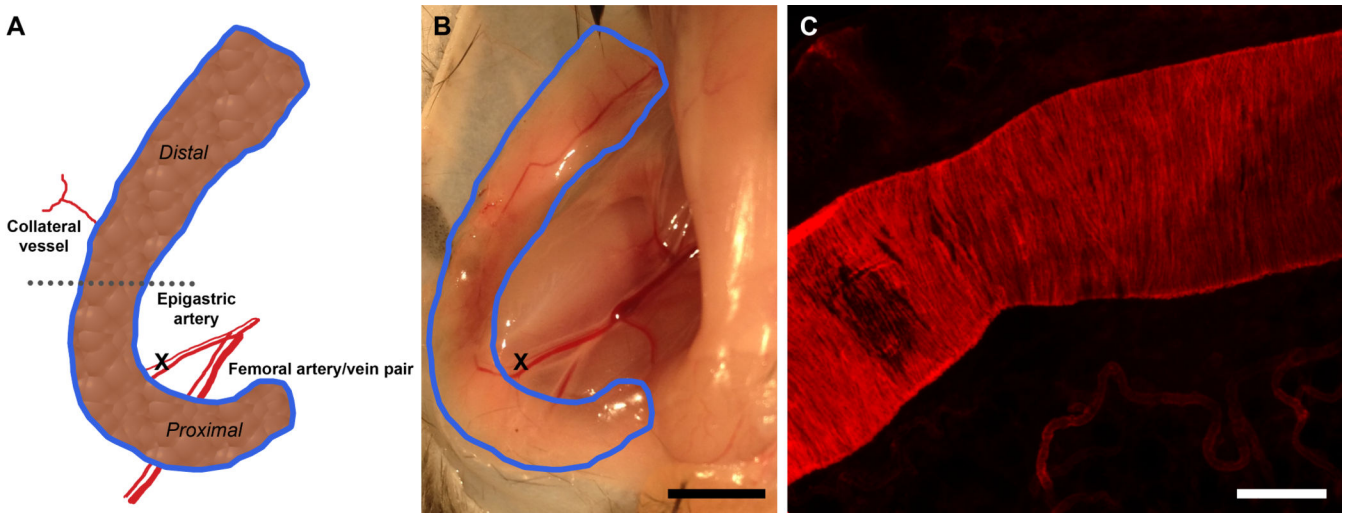

Figure 1.

In vivo murine model of flap delay. A.) Schematic of inguinal fat pad including epigastric artery (ligation site), femoral artery, collateral vessel, and areas of interest. B.) Macroscopic view of inguinal fat pad (outlined in blue) and ligation site. Scale bar = 5 mm. C.) Confocal micrograph of epigastric artery stained with α-smooth muscle actin. Scale bar = 100 μm.

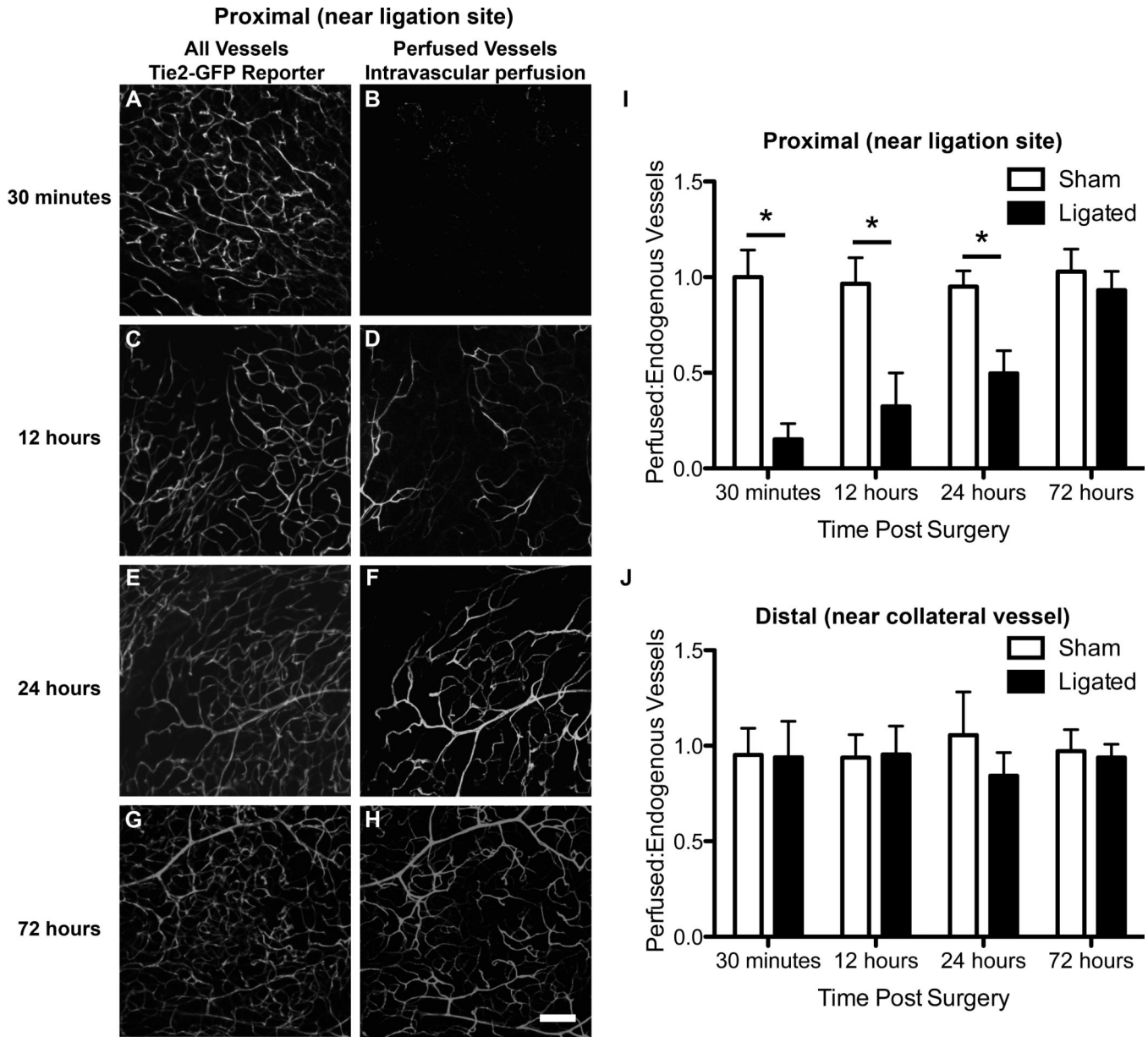

Figure 2.

Confocal micrographs reveal nearly complete flow recovery 72 hours post-ligation in the distal area. All vessels (A,C,E,G) are visualized using the Tie2-GFP mouse, while perfused vessels are visualized using isolectin intravascularly perfused (B,D,F,H). A,B.) All vessels and perfused vessels 30 minutes post-ligation. C,D.) Endogenous and perfused vessels 12 hours post-ligation. E,F.) Endogenous vessels and perfused vessels 24 hours post-ligation. G,H.) Endogenous and perfused vessels 72 hours post-ligation. I.) Quantification of perfusion to all vessels in the proximal region reveals a significant decrease in perfusion in ligated tissue 30 minutes, 12 hours, and 24 hours post-surgery (p-value < 0.05, Two-way ANOVA. J.) Quantification of perfusion to all vessels in the distal region reveals no significant decrease in perfusion in ligated tissue 30 minutes, 12 hours, and 24 hours post-surgery (p-value < 0.05, Two-way ANOVA. Three mice were used for each time point and

four FOVs were quantified. Scale bar = 100 μm. Data presented are mean + standard deviation for graphs.

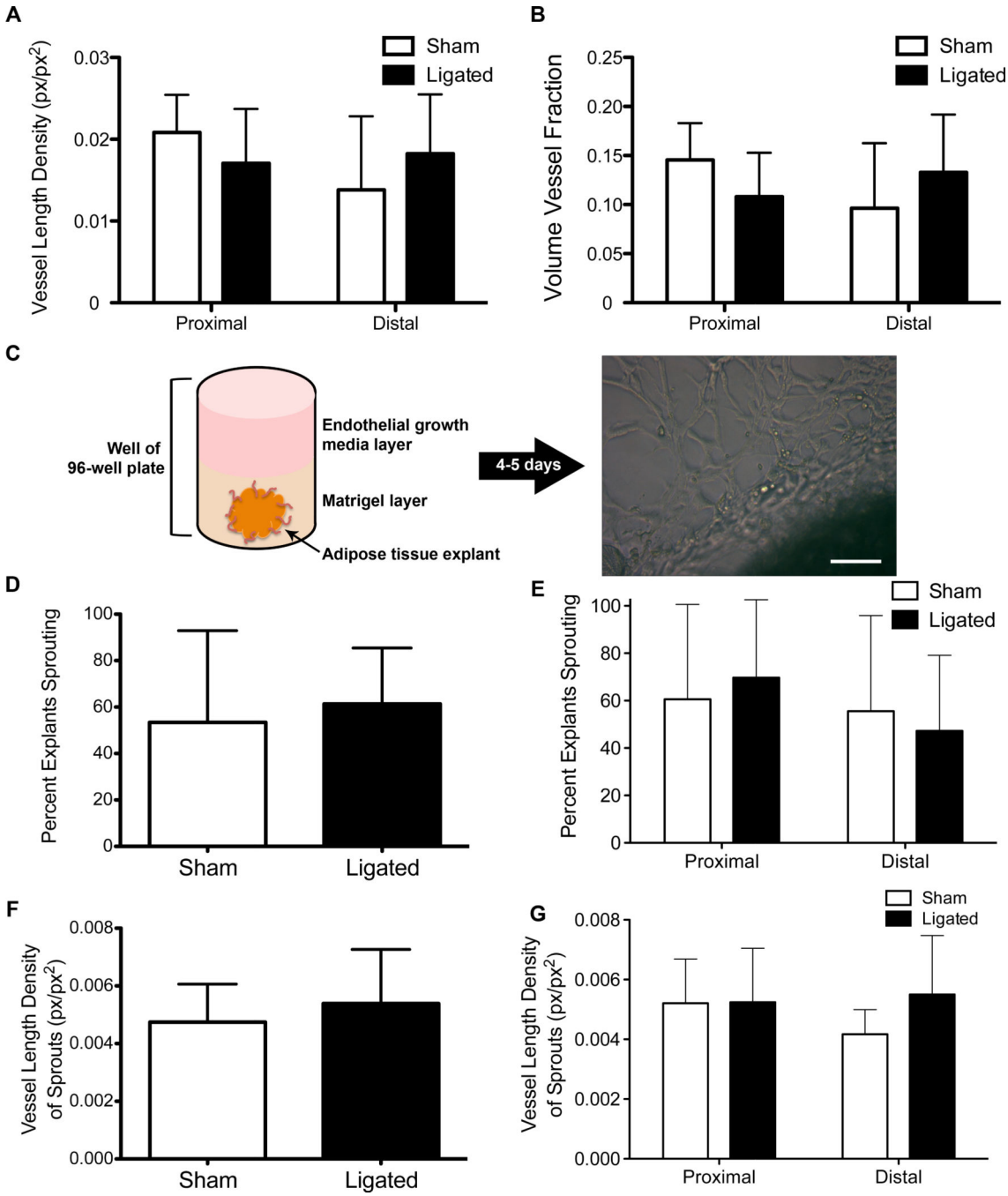

Figure 3.

No difference in angiogenic capability between sham and ligated tissue. En face visualization of adipose tissue and quantification using RAVE reveals no difference in VLD (A) or VVF (B). Three mice with four FOVs were used for calculation of VLD and VVF. Schematic of angiogenic capability assay (C) to assess sprouting prevalence (D,E) and vessel length density of sprouting events (F,G) in sham and ligated tissue by region of interest. Six mice were used and six samples were taken from each for use in the angiogenic

capability assay. Scale bar = 100 μm. p-value < 0.05, Two-way ANOVA. Data presented are mean + standard deviation for all graphs.

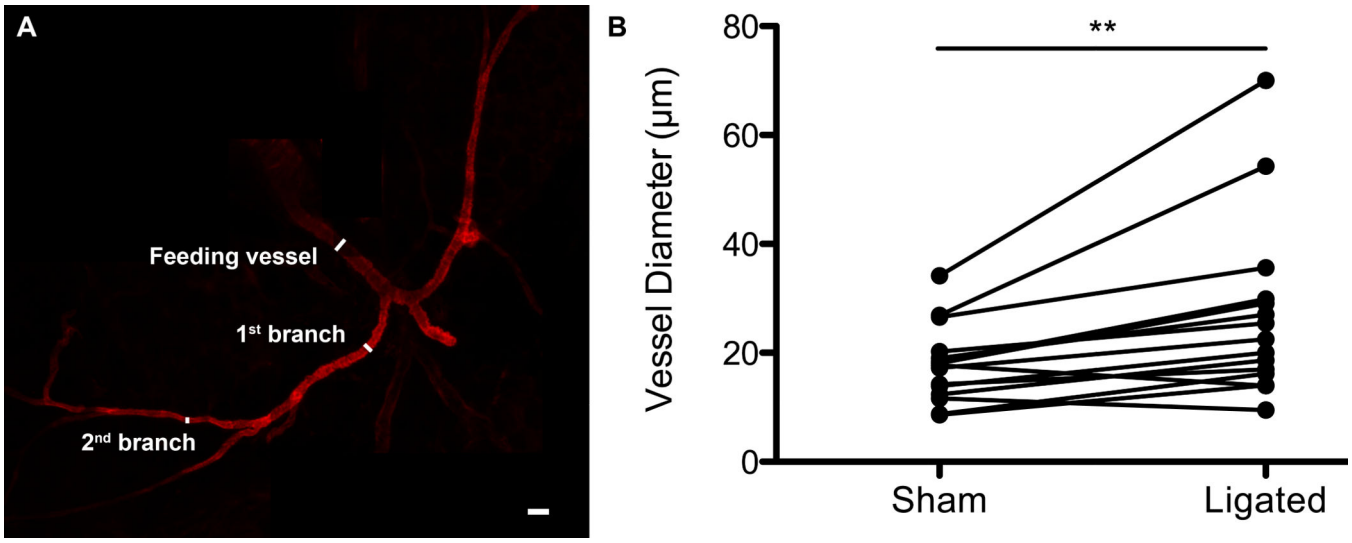

Figure 4.

Confocal micrographs of excised, structurally conserved collateral vessels reveal an increase in vessel diameter in ligated tissue when compared to paired sham tissue. A.) Excised collateral vessel stained with α-smooth muscle actin with feeding vessel, 1st branch, and 2nd branch identified. B.) Individual diameter measurements for sham tissues were paired with corresponding diameter measurements for ligated tissues (in the same mouse) and a paired t-test was run (p-value < 0.01). Five mice were used to quantify collateral vessel diameters. Scale bar = 50 μm.

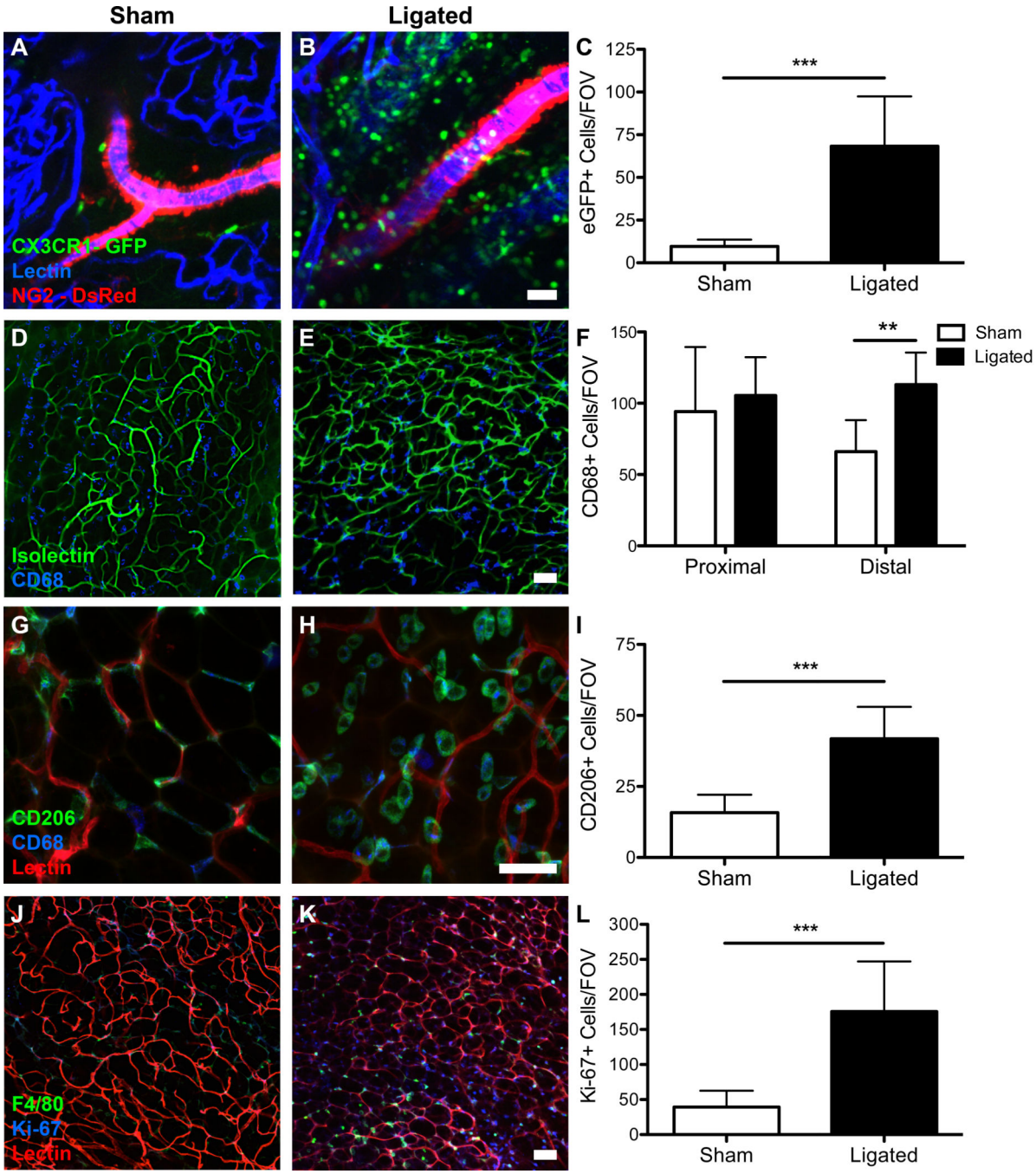

Figure 5.

Immunofluorescence staining reveals an increase in monocyte and macrophage recruitment to ligated tissue and an increase in proliferating cells in ligated tissue. A,B.) Confocal micrographs show an increase in CX3CR1-eGFP^{+} cells (green) in ligated tissue when compared to sham tissue. C.) Quantification of eGFP+ cells per FOV reveals an increase in eGFP+ cells in ligated tissue (p-value < 0.001, Student's t-test). Three mice were used and four FOVs were quantified. D,E.) Confocal micrographs show an increase in CD68^{+} cells (blue) in ligated tissue when compared to sham tissue. F.) Quantification of CD68^{+} cells per

FOV reveals an increase in $CD68^+$ cells in ligated tissue in the distal region (p-value<0.01, Two-way ANOVA). Three mice were used and four FOVs were quantified. G,H.) Confocal micrographs show an increase in $CD206^+$ cells (green) in ligated tissue when compared to sham tissue. I.) Quantification of $CD206^+$ cells per FOV reveals an increase in $CD206^+$ cells in ligated tissue in the distal region (p-value<0.001, Student's t-test). Three mice were used and four FOVs were quantified. J,K.) Confocal micrographs show an increase in Ki-67^+ cells (blue) in ligated tissue when compared to sham tissue. L.) Quantification of Ki-67^+ cells per FOV reveals an increase in Ki-67^+ cells in ligated tissue in the distal region (p-value<0.001, Student's t-test). Three mice were used and four FOVs were quantified. Scale bars = 50 μm. Data presented are mean + standard deviation for all graphs.